

CONSTRAINTS ON BYGONE NUCLEOSYNTHESIS OF ACCRETING NEUTRON STARS

ZACH MEISEL

Institute of Nuclear & Particle Physics, Department of Physics & Astronomy, Ohio University, Athens, Ohio 45701, USA and
Joint Institute for Nuclear Astrophysics – Center for the Evolution of the Elements, www.jinaweb.org

ALEX DEIBEL

Department of Physics & Astronomy, Michigan State University, East Lansing, Michigan 48824, USA and
Joint Institute for Nuclear Astrophysics – Center for the Evolution of the Elements, www.jinaweb.org*Draft version February 20, 2017*

ABSTRACT

Nuclear burning near the surface of an accreting neutron star produces ashes that, when compressed deeper by further accretion, alter the star's thermal and compositional structure. Bygone nucleosynthesis can be constrained by the impact of compressed ashes on the thermal relaxation of quiescent neutron star transients. In particular, Urca cooling nuclei pairs in nuclear burning ashes, which cool the neutron star crust via neutrino emission from e^- -capture/ β^- -decay cycles, provide signatures of prior nuclear burning over the \sim century timescales it takes to accrete to the e^- -capture depth of the strongest cooling pairs. Using crust cooling models of the accreting neutron star transient MAXI J0556-332, we show that this source likely lacked Type I X-ray bursts and superbursts $\gtrsim 120$ years ago. Reduced nuclear physics uncertainties in rp -process reaction rates and e^- -capture weak-transition strengths for low-lying transitions will improve nucleosynthesis constraints using this technique.

1. INTRODUCTION

Accreting neutron stars are unique probes of matter above nuclear saturation density and at low enough temperatures for quantum phenomena to emerge (Schatz & Rehm 2006). Accretion drives various nuclear burning processes near the neutron star surface that depend on the accretion rate and the composition of accreted material (Keek et al. 2014). Nuclear burning regimes include stable hydrogen burning (Schatz et al. 1999), unstable hydrogen burning in Type I X-ray bursts (Schatz et al. 1998; Woosley et al. 2004; Parikh et al. 2013), unstable carbon burning in superbursts (Strohmayer & Brown 2002; Schatz et al. 2003; Keek & Heger 2011), and each burning regime produces a characteristic nuclear abundance “ash” distribution. Further accretion compresses nuclear burning ashes deeper in the neutron star and drives further nuclear reaction sequences (Sato 1979) that replace the neutron star crust with processed ashes. As a result, the ocean and crust of an accreting neutron star have a thermal and compositional structure far different than the equilibrium state expected for an isolated neutron star composed of cold-catalyzed matter (Haensel & Zdunik 1990a).

Models of neutron star quasi-persistent transients are especially impacted by the details of accreted ashes. These neutron stars sporadically accrete matter from their accretion disks during \sim month to \sim year long outbursts. Active accretion drives nuclear reactions that deposit heat in the neutron star's ocean and crust (Haensel & Zdunik 1990b; Gupta et al. 2007), and the increase in temperature brings these layers out of thermal equilibrium with the core. When accretion ceases and the system enters quiescence, the neutron star ocean and

crust cool, and the surface thermal emission powers an X-ray light curve (Ushomirsky & Rutledge 2001; Rutledge et al. 2002). The cooling light curve reveals successively deeper layers with time and provides clues to the thermal and compositional profile as a function of depth (Brown & Cumming 2009; Page & Reddy 2013; Turlione et al. 2015).

The presence of Urca cooling, neutrino cooling via e^- -capture/ β^- -decay cycles between a pair of neutron-rich nuclides in an electron-degenerate environment (Gamow & Schoenberg 1941; Tsuruta & Cameron 1970), was recently identified in the crusts of accreting neutron stars (Schatz et al. 2014) and in the shallower ocean (Deibel et al. 2016b). Urca neutrino luminosities depend on the energy cost for e^- -capture, i.e. the Q -value, as Q_{EC}^5 , and the ambient temperature as T^5 . Urca neutrino cooling significantly impacts the thermal structure of neutron star crusts by acting as a high-temperature thermostat therein (Schatz et al. 2014; Deibel et al. 2015, 2016b). In principle, all neutron-rich nuclides with an odd number of nucleons A lead to some Urca cooling (Meisel et al. 2015; Deibel et al. 2016b), but the strength of Urca cooling depends on Urca nuclide abundances in the crust $X(A)$ and rates at which e^- -capture and β^- -decay proceed, which are quantified by weak-transition strengths $\log(ft)$ (Deibel et al. 2016b).

Here we demonstrate that Urca cooling in neutron star crusts reaching temperatures near $T \gtrsim 10^9$ K during active accretion has an observable impact on the quiescent light curve. In Section 2, we calculate Urca cooling neutrino luminosities using $X(A)$ from calculations of neutron star surface nucleosynthesis and $\log(ft)$ derived from experimental data. In Section 3, we add Urca cooling nuclei to a model of the quiescent thermal relaxation of the hot neutron star transient MAXI J0556-332, where the high crust temperature leads to strong Urca

cooling. Furthermore, we demonstrate that Type I X-ray bursts and superbursts on the accreting neutron star MAXI J0556-332 (Matsumura et al. 2011; Homan et al. 2014) $\gtrsim 120$ years ago can likely be excluded due to the impact Urca cooling would have on the quiescent light curve. We highlight further experimental work that is possible at present and near-future nuclear physics facilities that will improve these constraints in Section 4.

2. URCA COOLING NUCLEI PAIRS

When ashes of surface nuclear burning processes are buried by further accretion, they enter a degenerate electron gas whose Fermi energy E_F increases with depth. When $E_F \approx |Q_{EC}|$ for a given nucleus, where Q_{EC} is the electron-capture threshold energy, e^- -capture ensues that preserves the mass number A but changes the proton number Z to $Z - 1$ (Sato 1979). The finite-temperature environment enables e^- -capture to proceed when $|Q_{EC}| - k_B T \lesssim E_F \lesssim |Q_{EC}| + k_B T$, where k_B is the Boltzmann constant, and provides phase-space for the product of the e^- -capture reaction, i.e. daughter, to undergo β^- -decay within the same depth-window (Schatz et al. 2014). For cases in which the β^- -decay rate of the e^- -capture daughter is significant with respect to its e^- -capture rate, a condition which is fulfilled for all odd- A nuclides due to the monotonic increase of $|Q_{EC}(A)|$ for decreasing Z , an e^- -capture/ β^- -decay cycle can create an Urca pair. Pairs with significant weak-transition strengths, i.e. small $\log(ft)$, exhibit rapid cycling and consequently produce large neutrino luminosities. Layers in the crust that contain Urca cycling nuclei, denoted Urca shells, limit the heat transfer between regions above and below the Urca shell.

The neutrino luminosity for an Urca shell can be expressed as

$$L_\nu \approx L_{34} \times 10^{34} \text{ erg s}^{-1} X(A) T_9^5 \left(\frac{g_{14}}{2} \right)^{-1} R_{10}^2, \quad (1)$$

as derived in Tsuruta & Cameron (1970); Deibel et al. (2016b). Here $X(A)$ is the mass-fraction of the e^- -capture parent nucleus in the composition, T_9 is the temperature of the Urca shell in units of 10^9 K, $R_{10} \equiv R/(10 \text{ km})$, where R is the radius of the Urca shell from the neutron star center, and $g_{14} \equiv g/(10^{14} \text{ cm s}^{-2})$, where $g = (GM/R^2)(1 - 2GM/Rc^2)^{-1/2}$ is the surface gravity of the neutron star. The intrinsic cooling strength of the Urca pair, L_{34} , is given by

$$L_{34} = 0.87 \left(\frac{10^6 \text{ s}}{ft} \right) \left(\frac{56}{A} \right) \left(\frac{Q_{EC}}{4 \text{ MeV}} \right)^5 \left(\frac{\langle F \rangle^*}{0.5} \right), \quad (2)$$

where $\langle F \rangle^* \equiv \langle F \rangle^+ \langle F \rangle^- / (\langle F \rangle^+ + \langle F \rangle^-)$, the Coulomb factor $\langle F \rangle^\pm \approx 2\pi\alpha Z / |1 - \exp(\mp 2\pi\alpha Z)|$, and $\alpha \approx 1/137$ is the fine-structure constant.

We use values for L_{34} similar to those in Deibel et al. (2016b), which are based on Q_{EC} calculated using atomic mass excesses from Audi et al. (2012) and $\log(ft)$ based on experimental values when available; otherwise, $\log(ft)$ are obtained from Table 1 of Singh et al. (1998) using the experimentally determined ground state spin-parities J^π of the e^- -capture parent and daughter nuclides¹. We

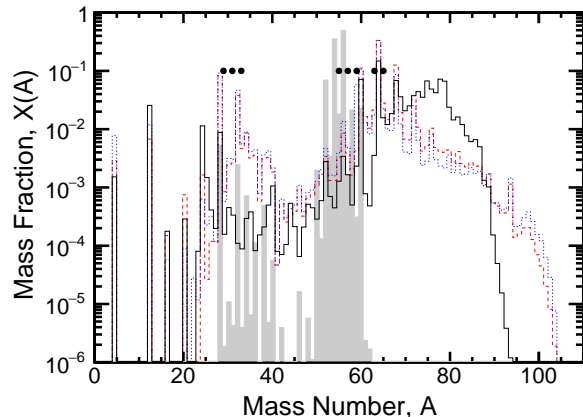


FIG. 1.— (color online.) Abundance distributions for ashes from model calculations of superbursts (gray-shaded histogram), stable burning (black histogram), and Type I X-ray bursts for a nominal nuclear reaction rate library (red-dashed histogram) and with the $^{59}\text{Cu}(p, \gamma)$ rate reduced by a factor of 100 (blue-dotted histogram) to demonstrate the sensitivity to nuclear reaction rates. The black filled-circles indicate mass-numbers with intrinsically strong Urca cooling strengths, according to Schatz et al. (2014).

opt for their (Singh et al. 1998) “Centroid” minus their “Width” for a given $\Delta J - \Delta\pi$, corresponding to a relatively fast, but plausible weak transition rate. This generally results in ft roughly one order of magnitude smaller than assumed in Deibel et al. (2016b), but one order of magnitude or more larger than the quasi-random phase approximation ft employed in Schatz et al. (2014).

We calculate the abundances of Urca pairs by modeling hydrogen and helium burning in the neutron star envelope, while relying on previous model calculations for carbon burning in the neutron star ocean. Type I X-ray burst and stable hydrogen burning ashes were calculated using the open-source software MESA (Paxton et al. 2011, 2013, 2015) version 8845. We primarily use parameters employed in Paxton et al. (2015) to reproduce Type I X-ray bursts from the source GS 1826-24 (Galloway et al. 2004; Heger et al. 2007), which produces bursts that undergo the full rp -process. Our model uses their (Paxton et al. 2015) 305-nucleus nuclear reaction network (with rates from REACLIB V2.0 (Cyburt et al. 2010)), an accreted composition with $X(^1\text{H}) = 0.72$, $X(^4\text{He}) = 0.26$, and 2% metals with a solar composition, and an envelope base luminosity $L = 1.6 \times 10^{34} \text{ ergs s}^{-1}$ (Woosley et al. 2004). Type I X-ray bursts were produced using an accretion rate $\dot{M} = 3 \times 10^{-9} \text{ M}_\odot \text{ yr}^{-1}$, while $\dot{M} = 4 \times 10^{-8} \text{ M}_\odot \text{ yr}^{-1}$ was chosen to reproduce stable hydrogen burning. $X(A)$ were extracted from the MESA results by averaging over ash layers with converged abundances and lacking any hydrogen or helium burning, as has been done in similar studies (Cyburt et al. 2016). We average over the ashes following 14 Type I X-ray bursts and for an equivalent burning time for the stable-burning ashes. $X(A)$ from Schatz et al. (2014) were adopted for superburst abundances and are based

file of experimental nuclear structure data maintained by the National Nuclear Data Center, Brookhaven National Laboratory (www.nndc.bnl.gov)—as of 2015 December 11.

¹ Evaluated Nuclear Structure Data File (ENSDF)—a computer

TABLE 1

PROPERTIES OF THE STRONGEST URCA e^- -CAPTURE REACTANT NUCLIDES, I.E. PARENTS, IDENTIFIED IN THIS WORK AND IN SCHATZ ET AL. (2014), ABSENT EVEN- A NUCLIDES, EXCLUDED BY MEISEL ET AL. (2015); DEIBEL ET AL. (2016b). TYPE I X-RAY BURST ASHES FROM THE MULTI-ZONE CALCULATIONS FROM CYBURT ET AL. (2016), AS WELL AS THE LAST BURST FROM MODELS 1 AND 2 OF JOSÉ ET AL. (2010) ARE INCLUDED FOR COMPARISON.

EC Parent	$ Q_{\text{EC}} $ (MeV)	$\log(ft)$	L_{34}	X_{SB}	X_{S}	$X_{\text{XRB}}^{\text{ThisWork}}$	$X_{\text{XRB}}^{\text{Cyburt,MZ}}$	$X_{\text{XRB}}^{\text{José,1}}$	$X_{\text{XRB}}^{\text{José,2}}$
^{29}Mg	13.3	5.1	8.2E+3	1.9E-6	1.6E-4	8.4E-4	1.8E-4	6.9E-4	6.7E-4
^{31}Al	11.8	4.9	4.2E+3	4.3E-6	3.4E-4	2.6E-3	2.8E-3	1.8E-3	1.4E-3
^{33}Al	13.4	5.2	3.7E+4	4.0E-6	8.8E-5	4.7E-3	5.2E-3	5.1E-3	2.4E-3
^{55}Sc	12.1	4.9	2.4E+3	1.8E-2	1.3E-3	3.3E-3	4.7E-3	5.3E-3	4.0E-3
^{57}Cr	8.3	11.6	8.6E-5	1.6E-3	1.7E-3	3.9E-3	4.1E-3	3.1E-3	3.4E-3
^{57}V	10.7	4.9	1.2E+3	1.6E-3	1.7E-3	3.9E-3	4.1E-3	3.1E-3	3.4E-3
^{59}Mn	7.6	11.6	5.2E-5	3.1E-4	2.3E-3	4.2E-3	4.5E-3	3.8E-3	3.7E-3
^{63}Cr	14.7	14.4	1.1E-6	6.5E-9	3.6E-3	2.1E-2	9.5E-3	3.3E-3	3.2E-3
^{65}Fe	10.3	11.6	2.1E-4	4.2E-12	1.6E-2	2.8E-2	1.5E-2	2.2E-3	3.1E-3
^{65}Mn	11.7	11.6	4.1E-4	4.2E-12	1.6E-2	2.8E-2	1.5E-2	2.2E-3	3.1E-3

on models described in Keek et al. (2012). Ash abundances are shown in Figure 1. Urca cooling neutrino luminosities were then calculated from $X(A)$ results for Type I X-ray bursts (X_{XRB}), superbursts (X_{SB}), and stable hydrogen burning (X_{S}); the 10 strongest Urca cooling pairs are listed in Table 1.

We demonstrate the sensitivity of our results to variations in rp -process nuclear reaction rates in Figure 1 by comparing to Type I X-ray burst ash abundances for a reduced $^{59}\text{Cu}(p, \gamma)$ reaction rate, which was one of the most influential rates for odd- A nuclide production identified by Cyburt et al. (2016). The sensitivity of our results to the X-ray burst model choice is demonstrated in Table 1 by comparison to ashes calculated from other multi-zone X-ray burst studies (José et al. 2010; Cyburt et al. 2016). We note that the X-ray burst ashes from Woosley et al. (2004) are substantially qualitatively different, where odd- A mass-fractions are orders of magnitude less than those found in our present calculations. Odd- A nuclide abundances are also substantially lower for the single-zone X-ray burst ashes of Cyburt et al. (2016).

3. CRUST COOLING WITH URCA PAIRS

We assess the impact of Urca cooling on the quiescent light curve of MAXI J0556-332 (“MAXI”). MAXI is one of a handful of accreting neutron star systems observed to date that have undergone an extended accretion outburst (\sim months) followed by a long quiescent period (\sim years) (Matsumura et al. 2011; Cornelisse et al. 2012; Homan et al. 2014). Among accreting neutron star transients, MAXI is exceptional due to the strong shallow heat source required to match observational data of the cooling light curve (Homan et al. 2014; Deibel et al. 2015). The inferred strong shallow heating results in a relatively large neutron star crust temperature, meaning that Urca shell neutrino luminosities would be especially large for this object if Urca nuclides were present in the crust. Furthermore, detection of hydrogen in the MAXI atmosphere indicates hydrogen comprises a significant fraction of the accreted material (Cornelisse et al. 2012). Therefore, MAXI is an ideal source to search for observational evidence of Urca cooling in the accreted neutron star crust.

We model the quiescent light curve of MAXI using

the open-source code **dStar** (Brown 2015; Deibel et al. 2015). **dStar** solves the general relativistic heat diffusion equation using the MESA numerical library (Paxton et al. 2011, 2013, 2015) for a neutron star crust using the microphysics of Brown & Cumming (2009); Deibel et al. (2015). We model the quiescent period of MAXI following a 480 day accretion outburst near the Eddington mass accretion rate $\dot{M}_{\text{Edd}} \approx 2 \times 10^{-8} M_{\odot} \text{ yr}^{-1}$ (Homan et al. 2014). Following the light curve fit from Deibel et al. (2015), the model uses a neutron star mass of $M = 1.5 M_{\odot}$, a neutron star radius of $R = 11 \text{ km}$, a crust impurity of $Q_{\text{imp}} = 1$, a core temperature of $T_{\text{core}} = 10^8 \text{ K}$, and a light-element envelope. In addition to heat-deposition from accretion, we include \dot{M} -dependent shallow heating over the pressure range $\log_{10}(P) = 28.2 - 28.6$ (with P in cgs units) inferred from the break in the MAXI light curve near $\approx 10-20$ days (Deibel et al. 2015), where the strength of the shallow heating Q_{sh} is adjusted to reproduce the light curve at early times. In past work, it was shown that the shallow heating strength must be between $Q_{\text{sh}} \approx 6-16 \text{ MeV}$ per accreted nucleon to match the hot surface temperature of MAXI J0556-332 at the outset of quiescence (Deibel et al. 2015). To investigate the impact of Urca cooling, we include an Urca shell at the e^- -capture depth for the strongest layer identified in Table 1, ^{33}Al , for which $X_{\text{XRB}}L_{34} \approx 160$ at a pressure $P_{\text{Urca}} \approx 3.6 \times 10^{26} \text{ erg cm}^{-3} (|Q_{\text{EC}}|/(3.7 \text{ MeV}))^4 \approx 6.2 \times 10^{28} \text{ g cm}^{-1} \text{ s}^{-2}$ (Deibel et al. 2016b).

Figure 2 shows the temperature as a function of depth for various times during active accretion with and without ^{33}Al Urca shell cooling for Type I X-ray burst ashes. Shallow and deep-crustal heating drive the crust out of thermal equilibrium with the core; however, the presence of an Urca shell limits the crust temperature by preventing shallow heating from diffusing to greater depths. This effect will impact the light curve at times $\gtrsim 20$ days, corresponding to thermal times at depths greater than the shallow heating source.

To reproduce the observations in the absence of Urca cooling, we choose a $Q_{\text{sh}} = 6 \text{ MeV}$ per accreted nucleon shallow heat source (Deibel et al. 2015). Note that we do not fit our crust parameters to the observational data, as the purpose of this work is to demonstrate the signature of Urca cooling on formerly accreting transients.

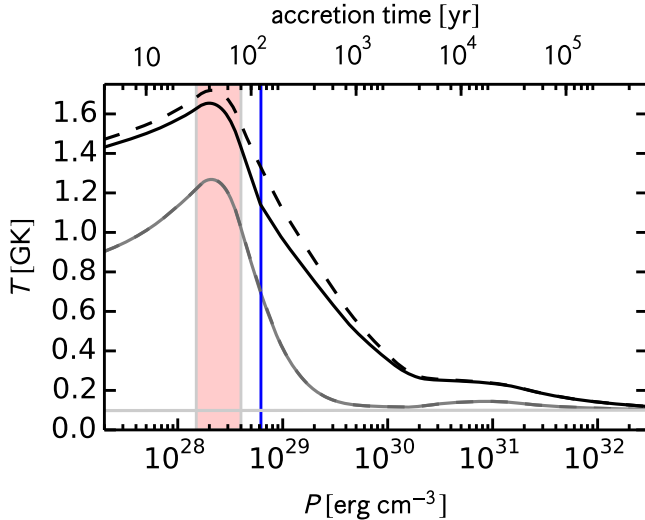


FIG. 2.— (color online.) Crust temperature profiles in MAXI, 0 days (light-gray lines), 48 days (gray lines), and 480 days (black lines) after the onset of an accretion outburst. Models with Urca cooling (solid lines) and without Urca cooling (dashed lines) are shown for the ^{33}Al Urca shell assuming Type I X-ray burst ash abundances. The red-shaded area and thin blue-line indicate the zones for shallow heating and Urca cooling, respectively.

When we include the ^{33}Al Urca shell in the crust cooling model, the predicted light curve shows a marked departure from the observations at early times. In particular, the light curve shape changes and dips below the observations between ≈ 10 days and $\approx 10^3$ days, before returning to a cooling trend that matches observations after $\gtrsim 10^3$ days. Note that the dip caused by the Urca cooling layer alters the shape of the light curve in a way that is difficult to compensate through changes in other neutron star parameters. We have, however, attempted to counteract the effect of Urca cooling by altering other model parameters as follows.

To compensate for the Urca cooling, we first increase Q_{sh} to 8 MeV per accreted nucleon, which restores the rough reproduction of observations out to tens of days, though a marked departure is still present ≈ 100 days after the end of accretion. One might expect this signature to disappear for higher crust impurities, as higher Q_{imp} will lengthen the thermal-diffusion timescale and effectively smear-out discrete features in the crust thermal profile (Brown & Cumming 2009; Page & Reddy 2013). Therefore, we adjust Q_{imp} to 100, likely the maximum plausible value (Schatz et al. 2001), but find the dip in the cooling light curve near 100 days persists. We find such a signature in the light curve is present for cooling strengths $\gtrsim 1/10^{\text{th}}$ our nominal $X_{\text{XRB}}L_{34}$ for ^{33}Al for an accreting transient with a crust temperature $\gtrsim 10^9$ K. Figure 4 highlights the signature of an Urca cooling layer on the transient light curve by showing the residual to our baseline *dStar* calculation. Substantially stronger cooling would be required to see the impact in a transient with a crust temperature near $\sim 10^8$ K, such as MXB 1659-29 (Brown & Cumming 2009; Deibel et al. 2016a), due to the T^5 -dependence of L_{ν} .

4. DISCUSSION

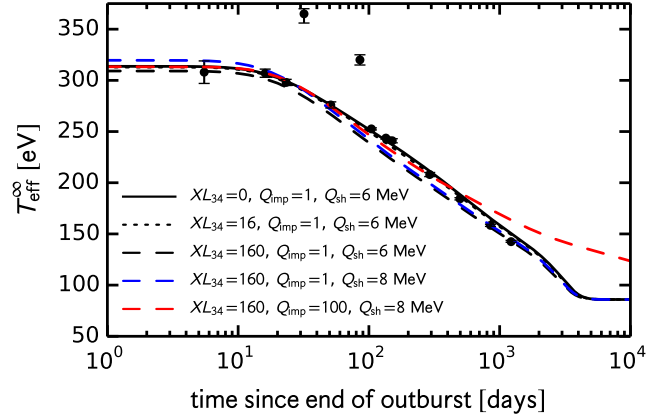


FIG. 3.— (color online.) Effective temperature of MAXI J0556-332 as a function of time for an observer at infinity. Crust cooling models are shown for various choices of the Urca cooling strength XL_{34} , crust impurity Q_{imp} , and shallow-heating strength Q_{sh} . Data points are from (Homan et al. 2014), except for two points near ~ 1000 days, which are preliminary (Aastha Parikh et al., in preparation).

We have examined the impact of Urca neutrino cooling on the predicted quiescent thermal relaxation of the hot neutron star transient MAXI J0556-332. Model light curves that include Urca cooling layers dip below the observations between ≈ 10 days and $\approx 10^3$ days, before returning to a cooling trend that matches observations after $\gtrsim 10^3$ days. As a result, to fit quiescent cooling observations, we find that MAXI must be absent of Urca cooling at the strength expected for Type I X-ray burst ashes at the depth at which ^{33}Al undergoes e^- -capture. We can also exclude Urca cooling from ^{55}Sc e^- -capture at the strength expected for superbust ash abundances, coincidentally at nearly the same depth, since this cooling is $\approx 1/3$ as strong. As such, we can constrain bygone nucleosynthesis on the surface of MAXI by calculating the time it would take for surface ashes to be buried to the depth of the ^{33}Al Urca shell.

For our calculations, the Urca shell depth of $P_{\text{Urca}} \approx 6.2 \times 10^{28} \text{ g cm}^{-1} \text{ s}^{-2}$ corresponds to a total accreted mass of $\approx 4.9 \times 10^{27} \text{ g}$, or ≈ 120 years of constant accretion at the inferred time-averaged outburst rate $\langle \dot{M} \rangle \approx \dot{M}_{\text{Edd}} \approx 2 \times 10^{-8} M_{\odot} \text{ yr}^{-1}$ (Homan et al. 2014). Therefore, we conclude that MAXI likely lacked Type I X-ray bursts and superbusts $\gtrsim 120$ years ago. Note that this is a lower limit that assumes MAXI has been constantly accreting at $\dot{M} = \dot{M}_{\text{Edd}}$ with a 100% duty cycle for the past 120 years. Our results are consistent with the near-Eddington accretion rate inferred for MAXI (Homan et al. 2014; Sugizaki et al. 2013), which implies stable nuclear burning of accreted material on the neutron star surface (Schatz et al. 1999; Keek & Heger 2016) and that the crust of MAXI J0556-332 is composed of stable burning ashes which have weak Urca cooling strengths. Furthermore, our results are consistent with the lack of observed Type I X-ray bursts for this source (Sugizaki et al. 2013) and provide an additional verification of the assumed accretion rate and the assumed distance for this source.

Surface nuclear burning at other timescales, such as Type I X-ray bursts at other accretion rates or different compositions of accreted material, could possibly be

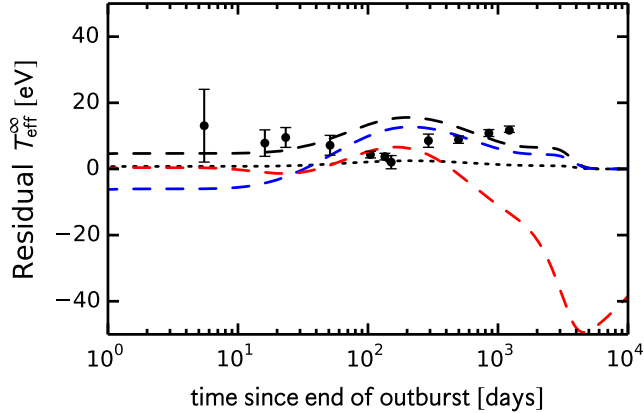


FIG. 4.— (color online.) Residuals for crust cooling models with Urca cooling in Figure 3 relative to the model calculation without Urca cooling assuming $XL_{34} = 0$, $Q_{\text{imp}} = 1$, and $Q_{\text{sh}} = 6$ MeV.

constrained using the technique presented here. The e^- -capture depths of the Urca pairs in Table 1 span accreted masses of $\sim 10^{26}$ – 10^{28} g, which correspond to surface nuclear burning ~ 2.5 –250 years ago for a neutron star with a 100% duty cycle accreting at $\dot{M} \sim \dot{M}_{\text{Edd}}$ and ~ 25 –2500 years for accretion rates $\dot{M} \sim 0.1 \dot{M}_{\text{Edd}}$ typical of Type I X-ray bursters (Galloway et al. 2008). Though many of the cooling strengths (XL_{34} in Table 1) are weak, future nuclear physics measurements and model calculations of surface nuclear burning may find stronger cooling. For varied accretion rates and nuclear reaction rates, X could be enhanced by several orders of magnitude, with the few-percent level as the empirical limit for odd- A (Schatz et al. 1999, 2001; Parikh et al. 2013; Cyburt et al. 2016). In addition, ft could be smaller by one or two orders of magnitude based on systematics (Singh et al. 1998). Future nuclear physics measurements of particular interest are rp -process reaction rates impacting the production of $A = 29, 31, 33, 55, 57, 59, 63$, and 65 , as well as $\log(ft)$ for low-lying transitions involved in e^- -capture on ^{31}Al , ^{33}Al , ^{55}Sc , ^{57}Cr , ^{57}V , ^{59}Mn , ^{63}Cr , ^{65}Fe , and ^{65}Mn . Such studies are possible via indirect measurements at present stable and radioactive ion beam facilities and direct measurements at near-future radioactive ion beam facilities.

The Urca cooling signature identified here in the light curves of cooling transients can be verified in the coming decades with continued monitoring of the X-ray sky by present telescopes such as MAXI², NUSTAR³, and ASTROSAT⁴, near-future telescopes such as NICER⁵, and planned telescopes such as LOFT⁶. In particular, identification of additional hot transients and long-term burst/burning monitoring for these sources would be most desirable.

In general, we find that Urca cooling in the crust has an observable impact on the light curves of transiently accreting neutron stars in quiescence whose crusts have achieved temperatures $\sim 10^9$ K for Urca nuclides with $X(A) \gtrsim 0.5\%$ and $\log(ft) \lesssim 5$. In particular, using $\log(ft)$ derived from experimental data and data-based systematics and $X(A)$ from model calculations of neutron star surface burning conditions, we exclude the existence of Type I X-ray bursts and superbursts $\gtrsim 120$ years ago for the source MAXI J0556-332. Modeling light curves of this and other neutron star transients with hot crusts after accretion turn-off can provide a window to examine the stability of surface nuclear burning on accreting neutron stars over millennia, improving constraints on the structure of accreted neutron star crusts.

We thank Laurens Keek for providing superburst ash abundances and Jeroen Homan for sharing the last two data points of the cooling curve of MAXI J0556-332 ahead of publication (Aastha Parikh et al., in preparation). Z.M. is supported by the Department of Energy under grant No. DE-FG02-88ER40387. A.D. is supported by the National Science Foundation under grant No. AST-1516969. We thank the International Space Science Institute in Bern, Switzerland for support received as a part of the International Team on Nuclear Reactions in Superdense Matter. We also thank the Department of Energy’s Institute for Nuclear Theory at the University of Washington for partial support during the completion of this work. This material is based on work supported by the National Science Foundation under grant No. PHY-1430152 (Joint Institute for Nuclear Astrophysics–Center for the Evolution of the Elements).

REFERENCES

- Audi, G., Wang, M., Wapstra, A. H., et al. 2012, *Chin. Phys. C*, 36, 2
- Brown, E., & Cumming, A. 2009, *Astrophys. J.*, 698, 1020
- Brown, E. F. 2015, *Astrophysics Source Code Library*, ascl:1505.034, <https://github.com/nwor/bde/dStar>
- Cornelisse, R., et al. 2012, *Mon. Not. R. Astron. Soc.*, 420, 3538
- Cyburt, R. H., Amthor, A. M., Heger, A., et al. 2016, *Astrophys. J.*, 830, 55
- Cyburt, R. H., et al. 2010, *Astrophys. J. Suppl. Ser.*, 189, 240
- Deibel, A., Cumming, A., Brown, E. F., & Page, D. 2015, *Astrophys. J. Lett.*, 809, L31
- Deibel, A., Cumming, A., Brown, E. F., & Reddy, S. 2016a, *arXiv:1609.07155*
- Deibel, A., Meisel, Z., Schatz, H., Brown, E. F., & Cumming, A. 2016b, *Astrophys. J.*, 831, 13
- Galloway, D. K., Cumming, A., Kuulkers, E., et al. 2004, *Astrophys. J.*, 601, 466
- Galloway, D. K., Muno, M. P., Hartman, J. M., Dimitrios, P., & Chakrabarty, D. 2008, *Astrophys. J. Suppl. Ser.*, 179, 360
- Gamow, G., & Schoenberg, M. 1941, *Phys. Rev.*, 59, 539
- Gupta, S., Brown, E. F., Schatz, H., Möller, P., & Kratz, K.-L. 2007, *Astrophys. J.*, 662, 1188
- Haensel, P., & Zdunik, J. L. 1990a, *Astron. & Astrophys.*, 229, 117
- . 1990b, *Astron. & Astrophys.*, 227, 431
- Heger, A., Cumming, A., Galloway, D. K., & Woosley, S. E. 2007, *Astrophys. J. Lett.*, 671, L141
- Homan, J., Fridriksson, J. K., Wijnands, R., et al. 2014, *Astrophys. J.*, 795, 131
- José, J., Moreno, F., Parikh, A., & Iliadis, C. 2010, *Astrophys. J. Suppl. Ser.*, 189, 204
- Keek, L., Cyburt, R. H., & Heger, A. 2014, *Astrophys. J.*, 787, 101
- Keek, L., & Heger, A. 2011, *Astrophys. J.*, 743, 189
- . 2016, *Mon. Not. R. Astron. Soc. Lett.*, 456, L11
- Keek, L., Heger, A., & in’t Zand, J. J. M. 2012, *ApJ*, 752, 150
- Matsumura, T., et al. 2011, *The Astronomer’s Telegram*, 3102, 1
- Meisel, Z., et al. 2015, *Phys. Rev. Lett.*, 115, 162501
- Page, D., & Reddy, S. 2013, *Phys. Rev. Lett.*, 111, 241102
- ² <http://maxi.riken.jp>
- ³ <http://www.nustar.caltech.edu>
- ⁴ <http://isro.gov.in/spacecraft/astrosat>
- ⁵ <https://www.nasa.gov/nicer>
- ⁶ <http://sci.esa.int/loft>

- Parikh, A., Jose, J., Sala, G., & Iliadis, C. 2013, *Prog. Part. Nucl. Phys.*, 69, 225
- Paxton, B., Bildsten, L., Dotter, A., et al. 2011, *Astrophys. J. Suppl. Ser.*, 192, 3, www.mesa.sourceforge.net
- Paxton, B., Cantiello, M., Arras, P., et al. 2013, *Astrophys. J. Suppl. Ser.*, 208, 4
- Paxton, B., Marchant, P., Schwab, J., et al. 2015, *Astrophys. J. Suppl. Ser.*, 220, 15
- Rutledge, R. E., Bildsten, L., Brown, E. F., et al. 2002, *Astrophys. J.*, 580, 413
- Sato, K. 1979, *Prog. Theor. Phys.*, 62, 957
- Schatz, H., Bildsten, L., & Cumming, A. 2003, *Astrophys. J. Lett.*, 583, L87
- Schatz, H., Bildsten, L., Cumming, A., & Wiescher, M. 1999, *Astrophys. J.*, 524, 1014
- Schatz, H., & Rehm, K. E. 2006, *Nucl. Phys. A*, 777, 601
- Schatz, H., et al. 1998, *Phys. Rep.*, 294
- Schatz, H., Aprahamian, A., Barnard, V., et al. 2001, *Phys. Rev. Lett.*, 86, 3471
- Schatz, H., et al. 2014, *Nature*, 505, 62
- Singh, B., Rodriguez, J. L., Wong, S. S. M., & Tuli, J. K. 1998, *Nuc. Data Sheets*, 84, 487
- Strohmayer, T. E., & Brown, E. F. 2002, *Astrophys. J.*, 566, 1045
- Sugizaki, M., et al. 2013, *Publ. Astron. Soc. Japan*, 65, 58
- Tsuruta, S., & Cameron, A. 1970, *Astrophys. Space Sci.*, 7, 374
- Turlione, A., Aguilera, D. N., & Pons, J. A. 2015, *Astron. & Astrophys.*, 577, A5
- Ushomirsky, G., & Rutledge, R. E. 2001, *Mon. Not. R. Astron. Soc.*, 325, 1157
- Woosley, S. E., Heger, A., Cumming, A., et al. 2004, *Astrophys. J. Suppl. Ser.*, 151, 75